Research Letter **DOI:** 10.15541/jim20240269

2D Plain and 3D Needle-punched C/SiC Composites: Low-velocity Impact Damage Behavior and Failure Mechanism

LUAN Xingang[1], HE Dianwei[1], TU Jianyong[2], CHENG Laifei[1]

(1. Science and Technology on Thermostructural Composite Materials Laboratory, Northwestern Polytechnical University, Xi'an 710072, China; 2. Xi'an Golden Mountain Ceramic Composites Co., Ltd., Xi'an 710118, China)

Abstract: Continuous carbon fiber reinforced silicon carbide (C/SiC) composites are often subjected to low-velocity impacts when utilized as structural materials for thermal protection. However, research on in-plane impact damage and multiple impact damage of C/SiC composites is limited. To investigate the in-plane impact damage behavior of C/SiC composites, a drop-weight impact test method was developed for strip samples, and these results were subsequently compared with those of C/SiC composite plates. Results show that the in-plane impact behavior of C/SiC strip samples is similar to that of C/SiC composite plates. Variation of the impact load with displacement is characterized by three stages: a nearly linear stage, a severe load drop stage, and a rebound stage where displacement occurs after the impact energy exceeds its peak value. Impact damage behavior under single and multiple impacts on 2D plain and 3D needled C/SiC composites was investigated at different impact energies and durations. Crack propagation in C/SiC composites was studied by computerized tomography (CT) technique. In the 2D plain C/SiC composite, load propagation between layers is hindered during impact, leading to delamination and 90° fiber brittle fracture. The crack length perpendicular to the impact direction increases with impact energy increases, resulting in more serious 0° fiber fracture and a larger area of fiber loss. In the 3D needled C/SiC composite, load propagates between the layers during impact through the connection of needled fibers. The fibers continue to provide substantial structural support, with notable instances of fiber pull-off and debonding. Consequently, the impact resistance is superior to that of 2D plain C/SiC composite. When the 3D needled C/SiC composite undergoes two successive impacts of 1.5 J, the energy absorption efficiency of the second impact is significantly lower, accompanied by a smaller impact displacement. Moreover, the total energy absorption efficiency of these two impacts of 1.5 J is lower than that of a single 3.0 J impact.

Key words: ceramic-matrix composite; fracture; low-velocity impact; computerized tomography analysis

Continuous C/SiC composites have the advantages of high strength, low weight, and excellent thermo-mechanical properties, making them ideal thermal structural materials for hypersonic vehicles[1-3]. However, the service environment of C/SiC composites is typically characterized by multi-field coupling effects, including stress, extremely high temperatures, and oxidizing agents. These factors significantly deteriorate the performance of C/SiC composites[4-6]. For example, the composites are inevitably subjected to the impact of falling weights and small stones during the preparation process and maintenance, which may affect their mechanical properties[7-8]. Although the velocity of these impacts is typically low, they can cause stress concentration[9], delamination elongation[10], durability degradation[11], and dynamic property changes[12], leading to non-negligible damage to C/SiC composites. Therefore, there are a large number of experimental studies and data simulations on low-velocity impact of composites[13-14]. Trabandt *et al.*[15] performed impact tests on C/SiC composites with chemical vapor deposition (CVD) coatings at impact energies of 0.7 and 1 J. It was found

Received date: 2024-06-03; **Revised date:** 2024-09-03; **Published online:** 2024-09-23
Foundation item: Aeronautical Science Foundation of China (2021Z057053001)
Biography: LUAN Xingang (1976–), male, PhD. E-mail: xgluan@nwpu.edu.cn
栾新刚(1976–), 男, 博士. E-mail: xgluan@nwpu.edu.cn
Corresponding author: LUAN Xingang, professor. E-mail: xgluan@nwpu.edu.cn;
TU Jianyong, senior engineer. E-mail: tujianyong1114@163.com
栾新刚, 教授. E-mail: xgluan@nwpu.edu.cn; 涂建勇, 高级工程师. E-mail: tujianyong1114@163.com

that there was no significant damage to C/SiC composites at the impact energy of 0.7 J, and the strength loss after impact was negligible, thus having little effect on the service life. Impacts greater than 1 J may cause damage to the composites. Mei *et al.*[16] found that C/SiC composite plates had good damage resistance to impacts with energy of 6 J and below. Additionally, proper low-velocity impact is beneficial for increasing the strength of C/SiC composites with appropriate dimensions by propagating cracks and weakening the interfacial bond, thereby eliminating all or part of the thermal residual stress. Liu *et al.*[17] found that U-shaped C/SiC composites with notch lines parallel to the needling direction had longer fiber pullout after low-velocity impacts, whereas U-shaped C/SiC composites with notch lines perpendicular to the needling direction had shorter fiber pullout after low-velocity impacts, showing significant delamination. Pi *et al.*[18] tested the residual tensile strength of 2D C/SiC-ZrC composites under different applied impact energies, investigated the damage characteristics and tensile properties after the impact by CT scanning method. Tita *et al.*[19] used load-time histories, displacement-time histories, as well as the images of an ultrasonic C-scan to verify the effects of low-velocity impact on the impact damage of thin C/SiC-ZrC composites.

In general, the key parameters of low-velocity impact are impact velocity, impact energy, sample shape, and sample stacking method. Although there are many studies on low-velocity and low-energy impact of C/SiC composites with different preform structures during or after a single impact, little attention has been paid to the impact direction or the impact times. For instance, these studies often consider only the direction perpendicular to fiber cloths for 2D plain C/SiC composite plates or a single impact in both directions for 3D needle-punched C/SiC composite plates. However, these two composites may be subjected to low-velocity impacts in the other directions during the service. For example, when a vehicle is impacted, its ribbed plate is subjected to a side impact as well. The impact resistance of ribbed plate after such an event remains uncertain. Therefore, it is necessary to examine the in-plane impact behavior of C/SiC thin plates, both under single and multiple impacts. We propose to develop a strip sample drop-weight impact test method and verify its consistency with the standard drop-weight impact test method. In this work, the low-velocity impact damage of a 2D C/SiC composite parallel to the fiber cloth direction and a 3D needle-punched C/SiC composite perpendicular to the needled fiber direction were investigated under different impact energies and impact times using notched C/SiC samples, and the foreign object debris/damage (FOD) mechanism of the samples was also investigated by CT and scanning electron microscope (SEM).

1 Experimental

1.1 Material preparation

C/SiC composites were prepared from T300 carbon fiber bundles (Toray Industries, Inc. Tokyo, Japan). The 2D fiber preform was formed by laminating 0°/90° plain fiber cloths layer by layer. The 3D fiber preform was made of 0° non-woven fiber cloth, 90° non-woven fiber cloth, short-cut fiber web, and needle-punched fiber bundles. The pyrolytic carbon (PyC, thickness of about 200 nm) was then introduced into the preforms as an interphase by chemical vapor infiltration (CVI) using a C_3H_6-Ar gas mixture. Eventually, the SiC matrix was prepared by CVI at 1000 ℃ using methyltrichlorosilane (MTS, CH_3SiCl_3) as the precursor. The C/SiC composites prepared by this process had a tensile stress of 320 MPa and a matrix cracking stress of 183 MPa[20].

The composite plates were cut into a sample with a size of 55 mm×10 mm×5 mm, followed by machining a notch with a depth of 5 mm and a bottom curvature radius of 1 mm. After that, a CVD SiC coating was applied to obtain the final sample, as shown in Fig. 1.

1.2 Impact test

Drop-weight impact testing of C/SiC composite strips was performed in accordance with ASTMD7136/D7136M. A drop-weight testing machine (Instron CEAST 9340) was used to perform the impact test. The end size of the drop ball is 16 mm in diameter. Before the start of the test, the sample was fixed under the drop weight using an independently designed mold. The impact energy was controlled by the height of the drop weight to be 1.0, 1.5, 2.0, and 3.0 J, at velocities of 0.72, 0.87, 1.00, and 1.22 m/s, respectively. The velocity sensor at the top of the impact ball of the drop weight was used to record the force and displacement of the sample during the process of impact.

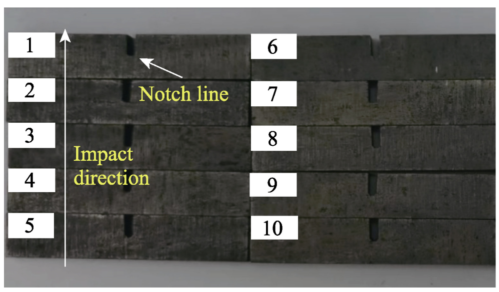

Fig. 1 Picture of notched samples

1.3 Impact damage detection

A scanning electron microscope (Tescan Clara GMH, Czech) was used to observe samples' fracture morphology to study the impact fracture mechanism of C/SiC composites with different preform structures. In order to study the energy-absorbing mode, a CT scanner (AX-2000, China) was used to observe the microstructural changes of the samples before and after impact.

2 Results and discussion

2.1 Effect of preform structure

To investigate the in-plane impact behavior of C/SiC composites, the drop-weight impact testing of C/SiC composite strips was conducted according to ASTMD7136/D7136M standard, with the results compared to those of drop-weight impact testing of C/SiC composite plates following the same standard[21]. Liu *et al.*[21] performed a low-velocity and low-energy impact on 2D laminated C/SiC composites and classified the variation of impact load with displacement into three phases: a nearly linear stage, a stage with severe load drop, and a stage where the displacement of the sample undergoes rebound after the impact energy exceeds its peak value. In this work, a similar displacement-load curve also appeared, exemplified by the 3D sample subjected to an impact energy of 1.5 J (Fig. 2(a)). The curve can be divided into three distinct stages: an almost linear stage (black in Fig. 2(a)), a stage characterized by a sharp drop in load (red in Fig. 2(a)), and a stage where the displacement springs back after the impact energy exceeds the peak value (blue in Fig. 2(a)). The above results indicate that it is feasible to study the in-plane impact damage behavior of C/SiC composites using the ASTMD7136/D7136M standard. Fig. 2(b) shows the energy-time curve of the sample. Initially, the energy increases almost linearly with time (black in Fig. 2(b)), after which the rate of increase decelerates to zero (red in Fig. 2(b)). At this point, the energy and sample displacement reach maximum. Subsequently, the sample begins to rebound, releasing a portion of the energy (blue in Fig. 2(b)).

The impact energy absorbed by the sample, E_a, is calculated by equation (1). In order to measure the absorption of energy during the impact of the sample, the ratio of the energy absorbed by the sample during the impact to the energy at the beginning of the impact is defined as the energy absorption efficiency (E_r), which is calculated according to equation (2).

$$E_a = mgh_1 + \frac{1}{2}mv_1^2 - mgh_2 - \frac{1}{2}mv_2^2 \tag{1}$$

$$E_r = \frac{E_a}{E_a + \frac{1}{2}mv_2^2} \tag{2}$$

Where m is weight of the sample, g is gravitational acceleration, h_1 and h_2 are heights before and after impact, v_1 and v_2 are velocities before and after impact.

The total energy absorbed by the sample (E_{ta}) and the total energy absorption efficiency of the sample subjected to two impacts (E_{tr}), are calculated for samples 3D-2×1.5J, by equations (3) and (4), respectively.

$$E_{ta} = mg(h_1 + h_3) + \frac{1}{2}m(v_1^2 + v_3^2) - mg(h_2 + h_4) - \frac{1}{2}m(v_2^2 + v_4^2) \tag{3}$$

$$E_{tr} = \frac{E_a}{E_a + \frac{1}{2}m(v_2^2 + v_4^2)} \tag{4}$$

Where h_3 and h_4 are heights before and after the second impact, v_3 and v_4 are velocities before and after the second impact.

The displacement of the punch at the end of the impact, Δh, is calculated by equation (5).

$$\Delta h = h_1(h_3) - h_2(h_4) \tag{5}$$

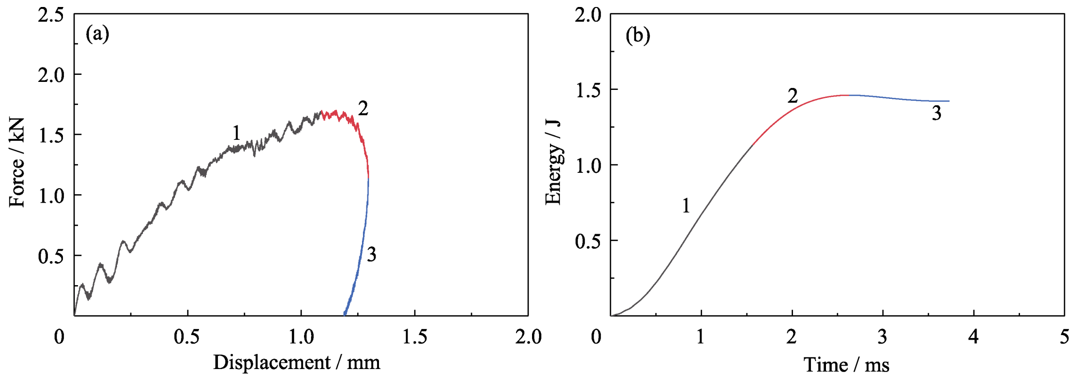

Fig. 2 Impact response of a 3D sample subjected to 1.5 J impact
(a) Displacement-load curve; (b) Energy-time curve. Colorful figures are available on website

Table 1 shows the impact energy absorption of the samples (impact energy absorption for all samples is given in Table S1). The 2D composite samples fracture at impacts of 1.0 J and above, their energy absorption efficiency decreases and displacement becomes larger as the impact energy increases. The 3D composite samples do not fracture at 1.5 J impact, they partially fracture at 3.0 J and repeated 1.5 J impacts. As the impact energy increases, the energy absorption efficiency decreases, and the displacement increases. For the 3D C/SiC composite subjected to twice impacts of 1.5 J, the energy absorption efficiency of the second impact is significantly reduced, with a smaller impact displacement.

The macroscopic morphology of the samples is shown in Fig. 3. Among the fractured samples, the 2D C/SiC composite exhibited delamination, while the 3D C/SiC composite, subjected to repeated 1.5 J impacts, demonstrated significant fiber pullout. The 2D C/SiC composite was all fractured under the impact energy of 1.0 J and above. The 3D C/SiC composites did not fracture at a single 1.5 J impact, while a portion of the 3D composite fractured at repeated 1.5 J impacts and a single 3.0 J impact. The 3D C/SiC composite demonstrated significantly better impact resistance than the 2D C/SiC composite, primarily due to its 3D needling structure, which allowed the fibers to perform a more effective load-bearing function compared to those in the 2D C/SiC composite.

Table 1 Energy absorption of sample

Sample	Impact energy/J	E_r/%	E_{tr}/%	Δh/mm	Case of sample fracture
2D	1.0	96.93		1.123	Broken
	1.5	96.01		1.379	Broken
	2.0	89.08		2.458	Broken
3D	1.5	96.98		1.155	Unbroken
	1.5(1)*	96.98	88.11	1.155	Unbroken
	1.5(2)*	80.55		0.724	Broken
	3.0	87.15		1.997	Unbroken
	3.0	91.54		1.873	Broken

*1.5(1) and 1.5(2) refer to the times of impact

Fig. 3 Macroscopic morphology of samples

From left to right, 2D-1.0J, 2D-1.5J, 2D-2.0J, 3D-1.5J, 3D-2×1.5J (broken), 3D-2×1.5J (unbroken), 3D-3.0J (broken), and 3D-3.0J (unbroken)

Fig. 4 shows the CT analysis results of phase and pore at 1 cm^3 near the U-shape of 2D and 3D C/SiC composites. The stacking direction of the 2D C/SiC fiber cloth is parallel to the notch line of the U-shape, and the direction of the sample subjected to impact is parallel to the fiber cloth. Additionally, Fig. 4(b3) shows that the needle-punched fibers are parallel to the notch line and perpendicular to the impact direction. Fiber volume fraction, matrix volume fraction, and porosity of the composites were calculated using the pore analysis module following CT analysis. Due to the fuzzy boundaries, the sum of the three volume fractions does not equal to 100%. The fiber volume fraction, matrix volume fraction, and porosity of 2D C/SiC composite are 41.74%, 50.70%, and 8.04%, respectively. These pores are mostly periodic larger pores with a volume of 30 mm^3. In contrast, the fiber volume fraction, matrix volume fraction, and porosity of 3D C/SiC composite are 41.99%, 50.33%, and 5.51%, respectively. These pores are variable in size and are mostly smaller, with a volume of 1 mm^3.

The energy-time curves and displacement-load curves of the sample under the impact energy of 1.5 J are shown in Fig. 5. By removing the gap elimination stage of sample 3D-1.5J-1 (the beginning of the energy-time curve and displacement-load curve of this sample), two patterns can be summarized. First, the 3D C/SiC composites exhibit a significantly faster energy rise in the linear stage and a shorter period of the stage where the load drops sharply. Additionally, it demonstrates greater energy recovery during the phase when the displacement rebounds after the impact energy exceeds the peak value. Second, the load-displacement curves of 3D C/SiC composites have larger peak loads and relatively smaller displacements, indicating that 3D C/SiC composite is more capable of transmitting forces.

In the CT photographs of the fractured samples after impact (Fig. 6), the 2D C/SiC composite is heavily delaminated, and the 3D C/SiC composite exhibits significant fiber pull-off.

Fig. 7 shows the fracture morphologies of the near U-shaped region of samples 2D-2.0J-1 and 3D-3.0J-1 after impact. It is evident that both 0° and 90° fibers in the 2D C/SiC composite have experienced significant fracture. Notably, the 90° fibers exhibit brittle fracture behavior, as shown in Fig. 7(b). The presence of large pores between 0° and 90° plain fiber cloths suggests the

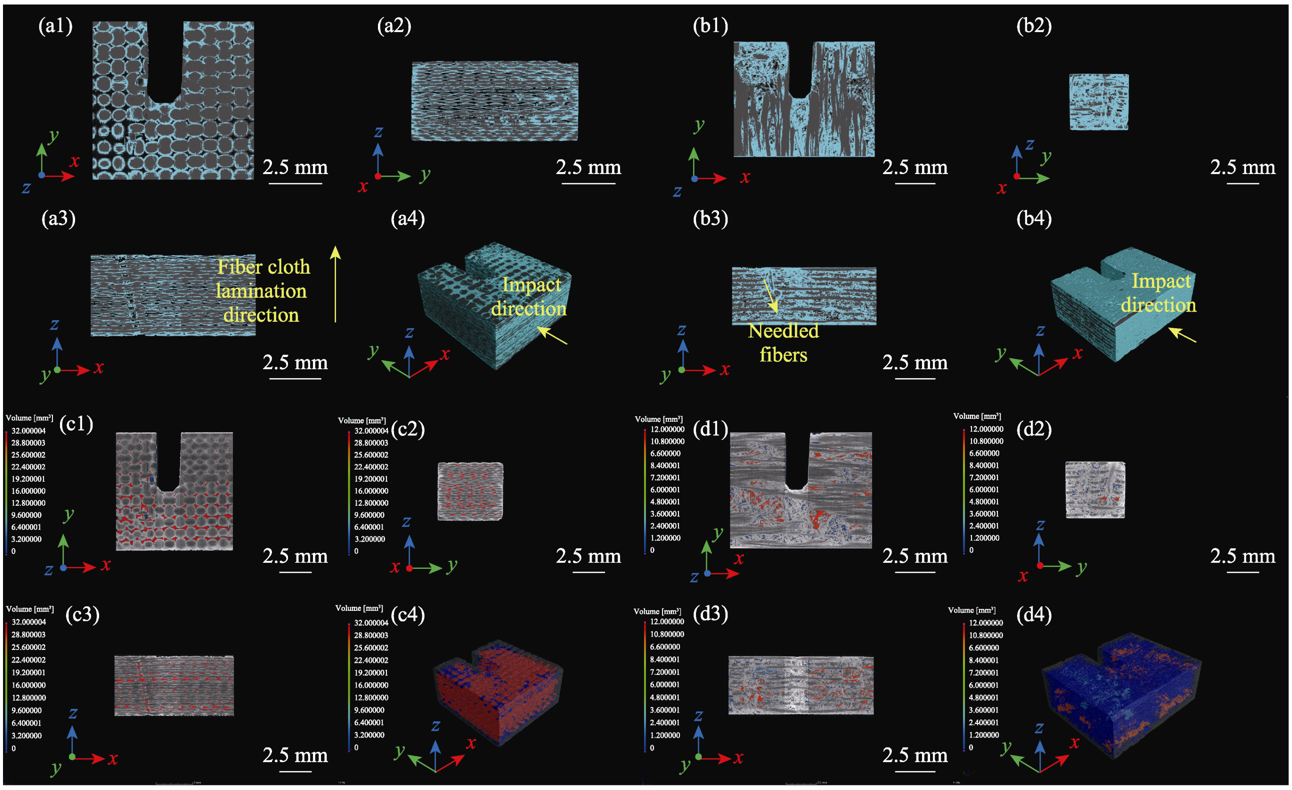

Fig. 4 Phase and pore analyses of samples using CT technique before impact

(Grey for C-fiber bundles, light blue for SiC matrix, red for large pores, dark blue for small pores)

Phase (a) and pore (c) analyses of the 2D C/SiC composite: (a1, c1) *XY* plane, (a2, c2) *YZ* plane, (a3, c3) *XZ* plane, and (a4, c4) stereogram; Phase (b) and pore (d) analyses of the 3D C/SiC composite: (b1, d1) *XY* plane, (b2, d2) *YZ* plane, (b3, d3) *XZ* plane, and (b4, d4) stereogram.

Colorful figures are available on website

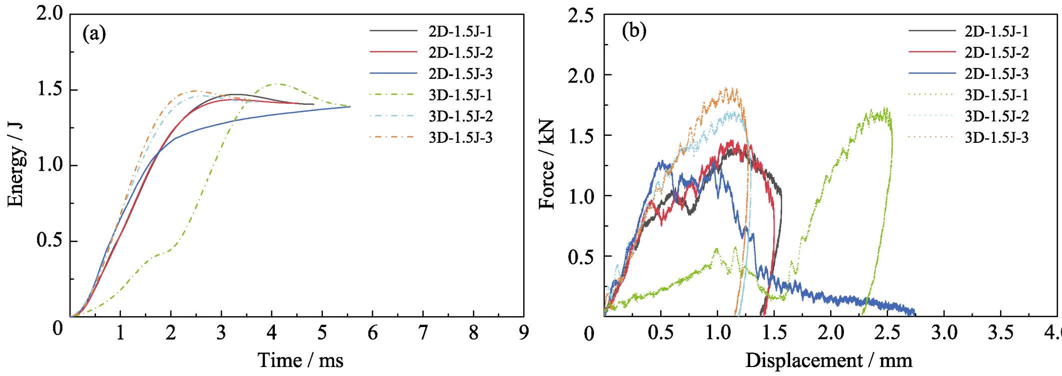

Fig. 5 (a) Energy-time curves and (b) displacement-load curves of samples at an impact energy of 1.5 J

Colorful figures are available on website

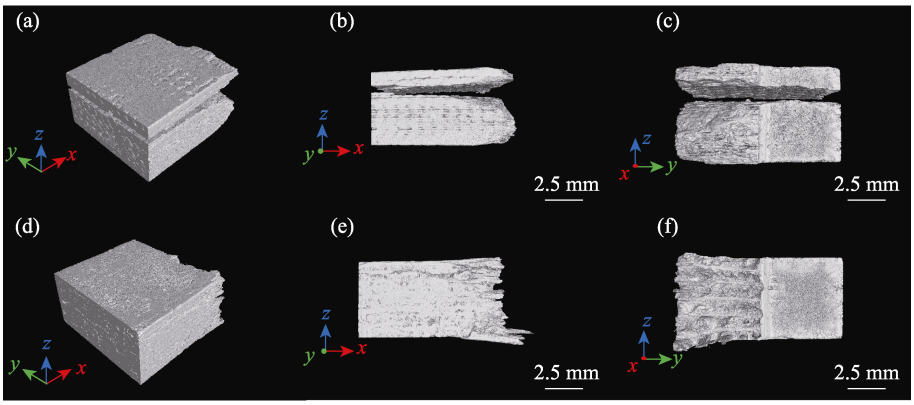

Fig. 6 CT photographs of the appearance of fractured C/SiC samples after impact

2D C/SiC composite: (a) stereoscopic view, (b) *YZ* plane, and (c) *XZ* plane;

3D C/SiC composite: (d) stereoscopic view, (e) *YZ* plane, and (f) *XZ* plane

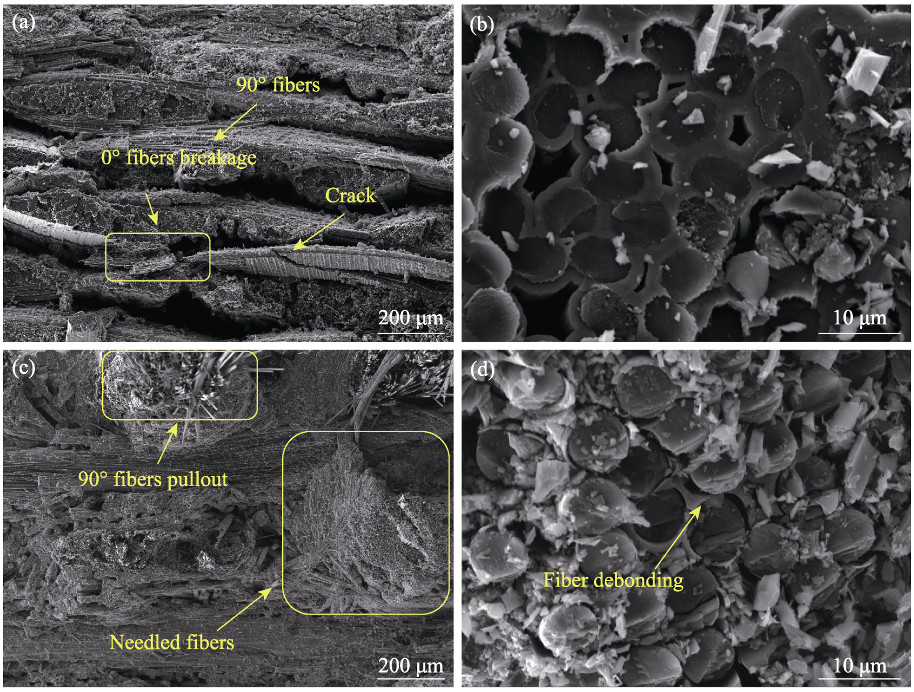

Fig. 7 Fracture morphologies of samples after impact
(a, b) Sample 2D-2.0J-1; (c, d) Sample 3D-3.0J-1

onset of interlayer damage in the 2D C/SiC composite. In the 3D C/SiC composite, the 90° fibers are obviously pulled out, accompanied by a debonding phenomenon. Additionally, the needle-punched fibers are connected between the 90° non-woven fiber cloth and the short-cut fiber web. In Fig. 7, a shape difference of fibers between 2D and 3D samples should be noticed, which is due to the different loading direction suffered by the fibers. Because of the poor shear strength of the C fiber in vertical direction, the fibers in the 2D C/SiC composite will be broken brittlely when suffering from the vertical impact. The 3D C/SiC composite has a certain load transfer capability due to the connecting function of the needled fibers, and the fibers are debonded and pulled out when the samples are impacted, which further consumes the energy brought by the impact.

The primary load-bearing component of the sample during impact is the 90° fiber perpendicular to the impact direction. Both 2D and 3D C/SiC composites have a fiber volume fraction of approximately 42%. Despite having similar 90° fiber volumes in their preform structures, they exhibit a significant difference in impact resistance. The morphologies depicted in Figs. 3, 4, 6, and 7, together with the energy-time and displacement-load curves in Fig. 5, reveal two key issues. First, for 2D C/SiC composite, load propagation between the two layers of the 2D plain preform during impact is hindered, leading to delamination and fracture. Second, 3D C/SiC composite exhibits some delamination phenomenon under the impact energy of 1.5 J. However, load transfer between layers is facilitated by the needled fibers, which maintain structural integrity. At an impact energy of 3.0 J, these fibers undergo pull-out and debonding.

2.2 Effect of impact times

The 3D composite was used to investigate the effect of impact times. For the 3D C/SiC composite subjected to repeated 1.5 J impacts, the energy absorption of the second impact is significantly reduced, with a smaller impact displacement. Consequently, the total energy absorption of the two impacts is lower than that of the single 3.0 J impact (Fig. 8).

CT scan results of the fracture area of the 3D C/SiC composite after impact are presented in Fig. 9. The main crack propagating in the *Y*-direction is visible in Fig. 9(a, d). The sample subjected to a 1.5 J impact exhibits delamination in the *Y*-direction (Fig. 9(b)), particularly near the 90° non-woven fiber cloth. In the sample subjected to a 3.0 J impact, the crack penetrates the 90° non-woven fibers (Fig. 9(e)). These observations indicate that 3D C/SiC composite did not fracture under either impact energy, though differences in the energy absorption mode are evident. The crack induced by the impact of 1.5 J is difficult to directly penetrate the 90° non-woven fibers, tending to offset upon reaching them, which leads to some delamination. As can be seen in Fig. 9(c, f), the crack propagation path in the sample subjected to a 3.0 J impact is significantly longer than that in the sample subjected to a 1.5 J impact, and the crack more clearly penetrates the 0° non-woven fibers.

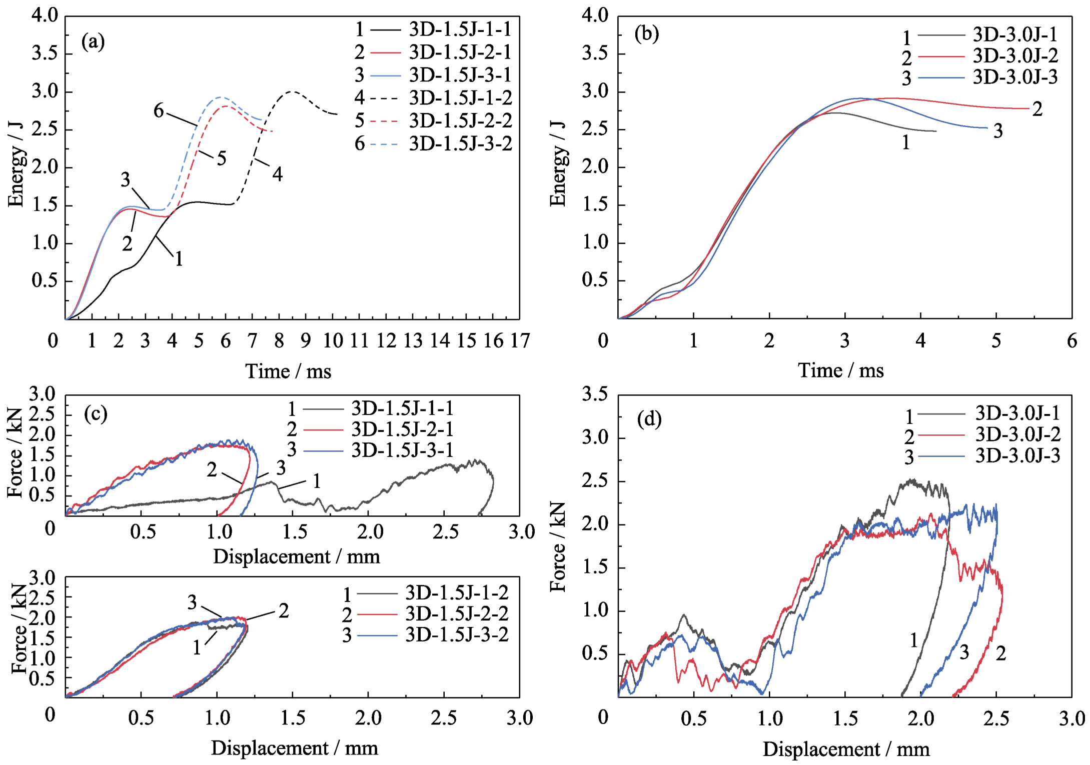

Fig. 8 Energy-time curves and displacement-load curves of 3D C/SiC composite with different impact energies

Energy-time: (a) 2×1.5 J and (b) 3.0 J; Displacement-load: (c) 2×1.5 J and (d) 3.0 J

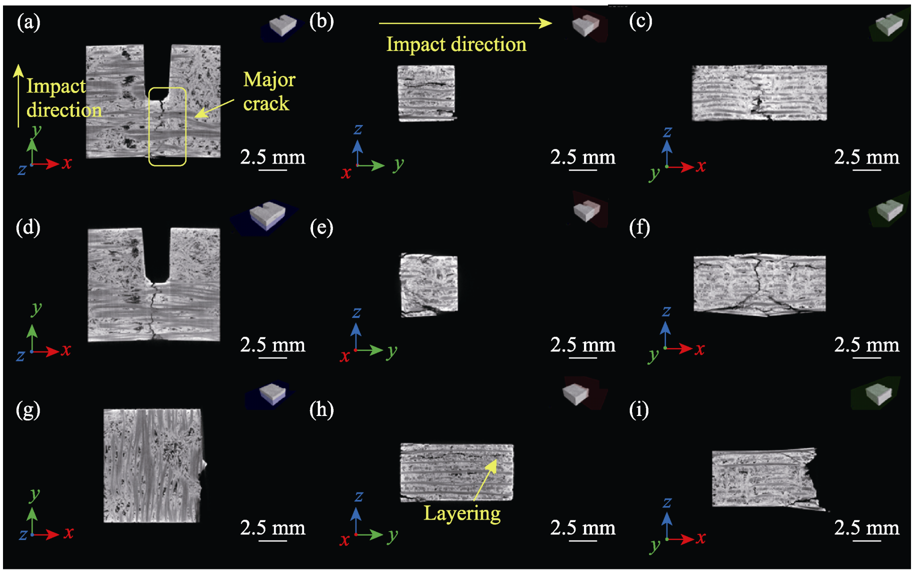

Fig. 9 CT scan results of 3D C/SiC composite after impact

XY plane: (a) 1.5 J, (d) 3.0 J, and (g) 2×1.5 J; *YZ* plane: (b) 1.5 J, (e) 3.0 J, and (h) 2×1.5 J; *XZ* plane: (c) 1.5 J, (f) 3.0 J, and (i) 2×1.5 J

2.3 Effect of impact energy

Energy-time curves and displacement-load curves of the 2D C/SiC composites with different impacts are shown in Fig. 10. At the end of the energy-time curves for samples 2D-1.5J-3 and 2D-2.0J-1–3, the energy is still increasing with time, and their displacement-load curves do not show a displacement rebound phase after the impact energy exceeds the peak value, indicating that the samples fracture without fully absorbing the energy of the drop weight. For the 2D C/SiC composite, the peak energy appears around 3 ms, and the slope of the energy-time curve increases in an approximately linear phase with the increase of the impact energy of the drop weight, indicating the increase of the energy absorption rate. With the increase of the impact energy, the displacements of the specimens also increase.

CT results of the fracture area of the 2D C/SiC composite after impact are shown in Fig. 11. All the samples exhibit a main crack in the *Y*-direction, which penetrates the sample. Additionally, significant damage is observed in the *X*- and *Z*-directions. The most serious damage occurs in the area where the sample first contacted the drop weight, as shown in Fig. 11(a, d, g). Cracks in the *Y*-direction can also be seen in Fig. 11(b, e, h). Notably, the sample subjected to a 2.0 J impact exhibits delamination. In Fig. 11(c, f, i), all samples exhibit large cracks in the *X*-direction. The sample subjected to a 2.0 J impact also has cracks penetrating in the *X*-direction, further indicating the delamination. Additionally, it is notable that the crack path in the *X*-direction is essentially parallel to the 0° fibers in the fiber cloth. In summary, the damage in the *X*- and *Y*-directions of the 2D sample reflects the layered fracture, and the damage in the *X*- and *Z*-directions of the sample, which are perpendicular to the impact direction, increases proportionally with impact energy.

The microscopic morphology of fractured 2D C/SiC composite is shown in Fig. 12. In Fig. 12(a), the 0° fibers are oriented perpendicular to the 90° fibers, with 0° fibers aligned parallel to the impact direction and the 90° fibers perpendicular to it. In Fig. 12(b-d), the 0° and 90° fibers break at a 1.0 J impact. As the impact energy increased, the 0° fibers of the sample broke more severely, accompanied by extensive fiber loss. The

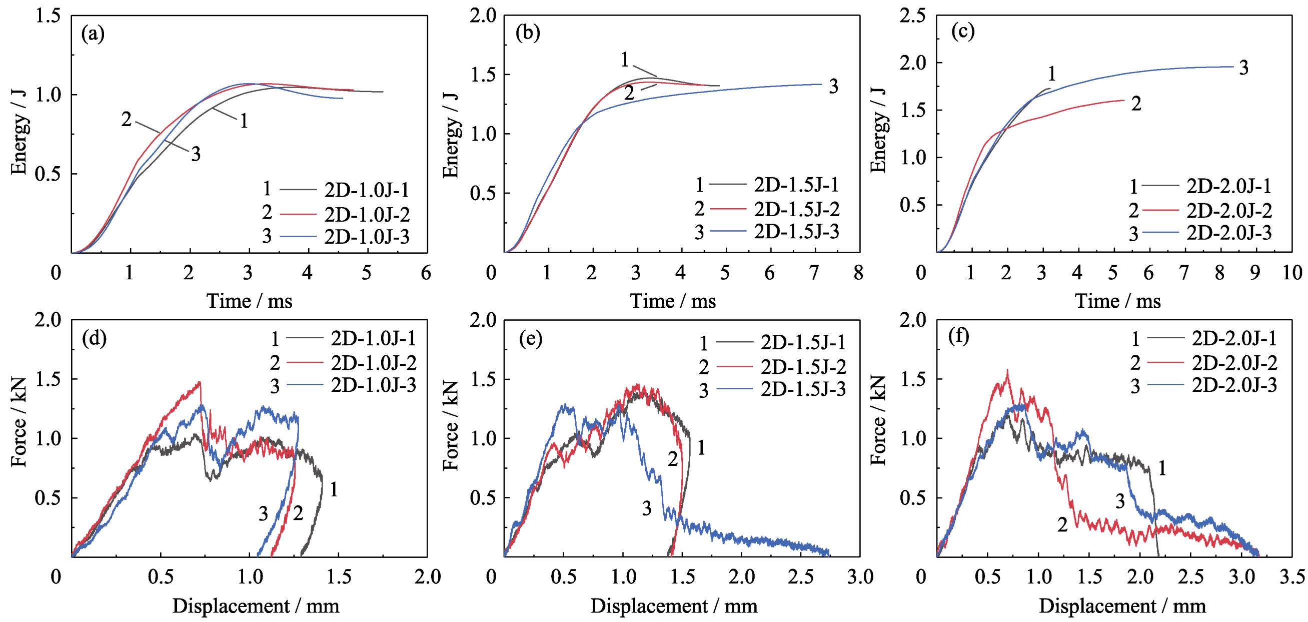

Fig. 10 Energy-time curves (a-c) and displacement-load (d-f) curves of 2D C/SiC composite with different impact energies of 1.0 J (a, d), 1.5 J (b, e), and 2.0 J (c, f)

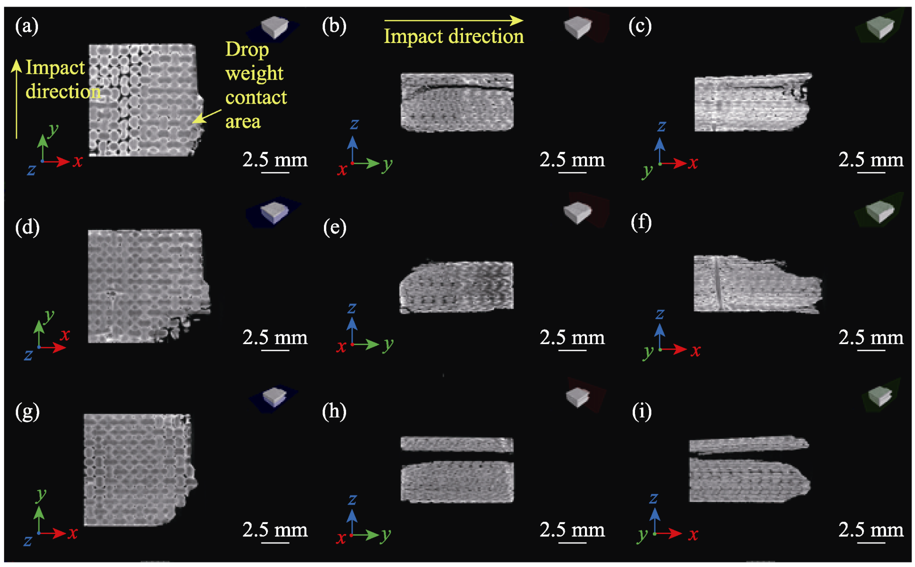

Fig. 11 CT scan results of 2D C/SiC composite after impact

XY plane: (a) 1.0, (d) 1.5, and (g) 2.0 J; *YZ* plane: (b) 1.0, (e) 1.5, and (h) 2.0 J; *XZ* plane: (c) 1.0, (f) 1.5, and (i) 2.0 J

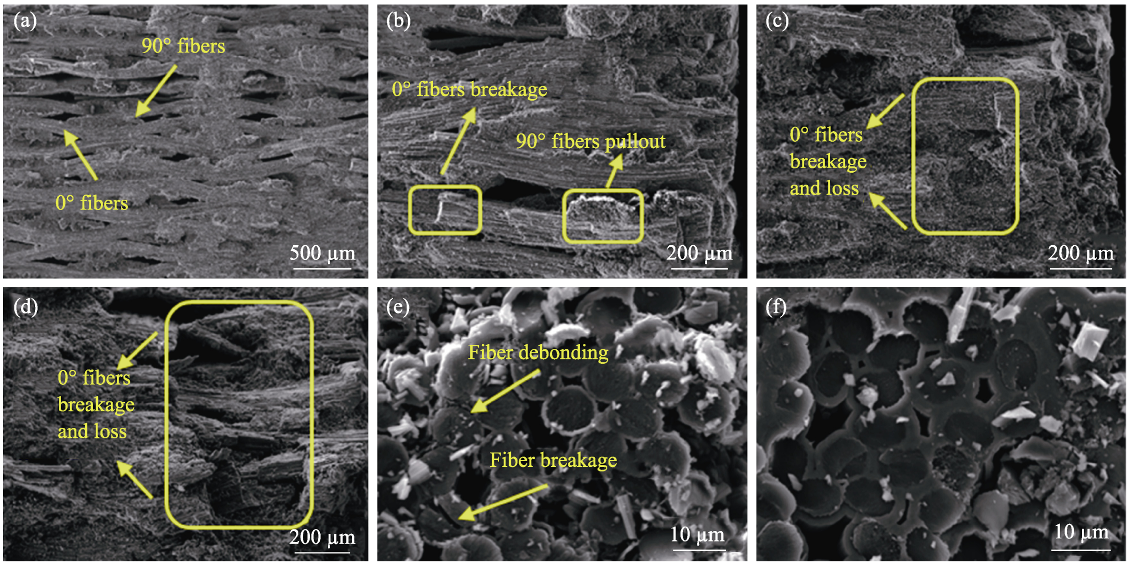

Fig. 12 Fracture morphologies of 2D C/SiC composite at different energies
(a, b, e) 1.0 J; (c) 1.5 J; (d, f) 2.0 J

consistent break heights of the 90° fibers suggest brittle fracture during impact. Notably, debonding of the 90° fibers and crack penetration are observed, as shown in Fig. 12(e).

3 Conclusions

The impact damage in C/SiC composites, particularly from low-velocity impacts, should not be underestimated. A 1.0 J impact can fracture a 2D U-shaped sample along the parallel fiber cloth stacking direction, whereas a single 3.0 J impact can fracture a 3D needled U-shaped sample along the perpendicular needled fiber direction. The crack length perpendicular to the impact direction extends with increasing impact energy. A 3D needled U-shaped sample subjected to either a single or double 1.5 J impacts demonstrates sufficient 90° fiber load capacity to deflect the crack and initiate delamination. In the 3D composite, the energy absorption modes for two 1.5 J impacts are slightly different from those for a single 3.0 J impact. The latter results in more efficient energy absorption, while the former induces more pronounced delamination. The 2D C/SiC composite exhibits delamination and brittle fracture upon impact, whereas the 3D C/SiC composite demonstrates superior impact resistance, evident by apparent fiber pullout upon fracture.

Supporting Materials

Supporting materials related to the article can be found at https://doi.org/10.15541/jim20240269.

References:

[1] ZHAO G C, JIANG Z G, QU Z L, *et al*. Fracture characteristics and *in-situ* damage mechanism of PIP-C/SiC composites to various temperatures and loading velocities. *Engineering Fracture Mechanics*, 2023, **286:** 109300.

[2] YAO L J, LI Z S, CHENG Q Y, *et al*. Damage behavior of 2D C/SiC composites under low velocity impact. *Journal of Inorganic Materials*, 2010, **25(3):** 311.

[3] YIN D Z, DENG Y F, MA Y Z, *et al*. Effect of SiC content on the mechanical behaviour of a three-dimensional needled C/SiC composite. *Ceramics International*, 2021, **47(17):** 25067.

[4] LI Y, XIAO P, SHI Y, *et al*. Mechanical behavior of LSI based C/C-SiC composites subjected to flexural loadings. *Composites Part A*, 2017, **95:** 315.

[5] NIU Z B, CHEN S A, LI Y, *et al*. A damage constitutive model for the nonlinear mechanical behavior of C/SiC composites during mechanical cyclical loading/unloading. *Composites Part A*: *Applied Science and Manufacturing*, 2022, **161:** 107072.

[6] ALMEIDA R S M, CHEN S A, BESSER B, *et al*. Fatigue behavior and damage analysis of PIP C/SiC composite. *Journal of the European Ceramic Society*, 2022, **42(13):** 5391.

[7] YAO L J, LYU P, BAI G D, *et al*. Influence of low velocity impact on oxidation performance of SiC coated C/SiC composites. *Ceramics International*, 2019, **45(16):** 20470.

[8] MEI H, YU C K, XU H R, *et al*. The effects of stitched density on low-velocity impact damage of cross-woven carbon fiber reinforced silicon carbide composites. *Ceramics International*, 2016, **42(1):** 1762.

[9] FRANKEL P G, WITHERS P J, PREUSS M, *et al*. Residual stress fields after FOD impact on flat and aerofoil-shaped leading edges. *Mechanics of Materials*, 2012, **55:** 130.

[10] KHARGHANI N, SOARES C G. Behavior of composite laminates with embedded delaminations. *Composite Structures*, 2016, **150:** 226.

[11] SINGH A, MALL S. Tensile and fatigue behavior of oxide/oxide ceramic matrix composite with simulated foreign object damage in combustion environment. *International Journal of Applied Ceramic Technology*, 2017, **15(1):** 16.

[12] ESPINO N V. Prediction of foreign object debris/damage (FOD)

type for elimination in the aeronautics manufacturing environment through logistic regression model. Texas: The University of Texas at El Paso, Master's thesis, 2013.

[13] CHEN X. Foreign object damage on the leading edge of a thin blade. *Mechanics of Materials*, 2005, **37(4):** 447.

[14] DING J, HALL R F, BYRNE J, *et al*. Fatigue crack growth from foreign object damage under combined low and high cycle loading. Part I: experimental studies. *International Journal of Fatigue*, 2007, **29(7):** 1339.

[15] TRABANDT U, ESSER B, KOCH D, *et al*. Ceramic matrix composites life cycle testing under reusable launcher environmental conditions. *International Journal of Applied Ceramic Technology*, 2005, **2(2):** 150.

[16] MEI H, YU C K, XU Y W, *et al*. Effect of impact energy on damage resistance and mechanical property of C/SiC composites under low velocity impact. *Materials Science and Engineering: A*, 2017, **687:** 141.

[17] LIU B, AN Q J, ZHONG J G, *et al*. Study on notch sensitivity and failure of 3D needled C/SiC fracture toughness. *Advances in Aeronautical Science and Engineering*, 2022, **13(2):** 85.

[18] PI H L, ZHANG B P, YU X M, *et al*. Damage characteristics of 2D C/SiC-ZrC composites under low velocity impact. *Journal of Inorganic Materials*, 2020, **35(12):** 1327.

[19] TITA V, DE CARVALHO J, VANDEPITTE D. Failure analysis of low velocity impact on thin composite laminates: experimental and numerical approaches. *Composite Structures*, 2008, **83(4):** 413.

[20] ZHAO D L, GUO T, FAN X M, *et al*. Effect of pyrolytic carbon interphase on mechanical properties of mini T800-C/SiC composites. *Journal of Advanced Ceramics*, 2021, **10(2):** 219.

[21] LIU B, GAO Y D, TAN Z Y, *et al*. Low energy level impact damage on 2D C/SiC composites: experimental study. *Acta Aeronautica et Astronautica Sinica*, 2021, **42(2):** 224202.

2D 平纹和 3D 针刺 C/SiC 复合材料的低速冲击破坏行为和失效机理

栾新刚[1], 何典蔚[1], 涂建勇[2], 成来飞[1]

(1. 西北工业大学 超高温结构复合材料重点实验室, 西安 710072; 2. 西安金山瓷业有限公司, 西安 710118)

摘 要: 连续碳纤维增强碳化硅(C/SiC)复合材料用作热防护结构材料时, 可能遭受低速冲击损伤。然而, 目前对于 C/SiC 复合材料面内冲击损伤和多次冲击损伤的研究尚不充分。本研究通过落锤冲击试验, 测试了 C/SiC 条状试样的面内冲击破坏行为, 并与 C/SiC 复合板的落锤冲击试验进行了比较。结果表明, C/SiC 条状试样的面内冲击行为与 C/SiC 复合板相似, 冲击载荷随位移的变化可分为三个阶段: 近似线性阶段、载荷骤降阶段、冲击能量超过峰值后试样位移发生反弹阶段。对二维(2D)平纹 C/SiC 复合材料和三维(3D)针刺 C/SiC 复合材料在不同冲击能量和时间下的单次和多次冲击破坏行为进行了研究。借助计算机断层扫描(CT)技术研究了 C/SiC 复合材料的裂纹扩展。对于 2D 平纹 C/SiC 复合材料, 冲击过程中载荷难以在预制体的层间传播, 导致分层和 90°纤维脆性断裂。随着冲击能量增大, 垂直于冲击方向的裂纹长度增加, 0°纤维断裂加剧, 纤维损失面积增大。对于 3D 针刺 C/SiC 复合材料, 冲击过程中载荷通过针刺纤维的连接在层间传播, 纤维依然起到良好的支撑作用, 出现纤维拉断和脱黏现象, 其抗冲击性能优于 2D 平纹 C/SiC 复合材料。对于受到两次 1.5 J 冲击的 3D 针刺 C/SiC 复合材料, 第二次冲击的能量吸收率明显降低, 冲击位移减小, 两次 1.5 J 冲击的总能量吸收效率低于单次 3.0 J 冲击。

关 键 词: 陶瓷基复合材料; 断裂; 低速冲击; 计算机断层扫描分析

中图分类号: TB332 **文献标志码:** A **文章编号:** 1000-324X(2025)02-0205-10

Supporting information:

2D Plain and 3D Needle-punched C/SiC Composites: Low-velocity Impact Damage Behavior and Failure Mechanism

LUAN Xingang[1], HE Dianwei[1], TU Jianyong[2], CHENG Laifei[1]

(1. Science and Technology on Thermostructural Composite Materials Laboratory, Northwestern Polytechnical University, Xi'an 710072, China; 2. Xi'an Golden Mountain Ceramic Composites Co., Ltd., Xi'an 710118, China)

Table S1 Impact energy absorption for all samples

Sample	Number	Impact energy/J	E_r/%	E_{tr}/%	Δh/mm	Case of sample fracture
2D	1	1.0	97.69		1.289	Broken
	2	1.0	96.93		1.123	Broken
	3	1.0	92.13		1.045	Broken
	1	1.5	96.01		1.379	Broken
	2	1.5	98.58		1.410	Broken
	3	1.5	93.67		2.737*	Broken
	1	2.0	80.79		3.175	Broken
	2	2.0	98.69		3.166	Broken
	3	2.0	89.08		2.458	Broken
3D	1	1.5	91.35		2.277	Unbroken
	2	1.5	97.58		1.188	Unbroken
	3	1.5	96.98		1.155	Unbroken
	1	1.5	98.15	89.72	2.725*	Unbroken
		1.5	80.88		0.754	Broken
	2	1.5	93.60	86.01	1.008	Unbroken
		1.5	78.36		0.712	Unbroken
	3	1.5	96.98	88.11	1.155	Unbroken
		1.5	80.55		0.724	Broken
	1	3.0	95.73		2.212	Unbroken
	2	3.0	87.15		1.997	Unbroken
	3	3.0	91.54		1.873	Broken

*These displacement results are not used, because these results include testing error, according to the energy-displacement curves